DNA Nanomechanical Switches under Folding Kinetics Control

Virgile Viasnoff,[†,‡] Amit Meller,[‡] and Hervé Isambert*,[†]

*Physico-chimie Curie, CNRS UMR168, Institut Curie, Section de Recherche,
11 rue P. & M. Curie, 75005 Paris, France, and Rowland Institute at Harvard,
Harvard University, 100 Edwin H. Land Boulevard, Cambridge, Massachusetts 02142*

ABSTRACT

Existing DNA nanodevices operate at equilibrium under changes in solution composition. We propose an alternative DNA switch design that can be driven and maintained out of equilibrium, under *fixed* chemical conditions. Moderate cooling rate after heat denaturation drives the switch to its lowest energy conformation, while rapid cooling (>100 °C/ms) locks the molecule in a unique alternative conformation that is retained over weeks at room temperature. This reversible process is probed using fluorescent energy transfer. DNA switches operating out of equilibrium should be more amenable to nanotechnology applications and scalable integration.

The design of nanoscale switchable devices is one of the goals of nanotechnology, as the prospect of controlling nanomechanical devices and molecular switches stands at the core of many promising applications.[1−4] Beyond its central role in biology, DNA has long been recognized as a versatile molecule that can self-assemble into nanoscale objects[5−8] or form well-controlled supramolecular scaffolds.[9−11] More recently, DNA was also shown to provide switchable nanomechanical devices whose *equilibrium* states can be controlled by changing, for example, the medium ionic strength[12] or by using additional "fuel" and "waste" DNA molecules.[13−18] We present the simple alternative design of a generic DNA switch controlled by the rate of temperature variation, under fixed chemical conditions. Slow or fast renaturation cycles rapidly and reversibly interchange its two conformations, while their spontaneous equilibration can take several weeks at room temperature through nucleation and branch migration of a Holliday junction.

The two structures of the DNA nanomechanical switch, corresponding to contracted and elongated conformations, are constructed around the repeat of a 14 nt region P and its complementary sequence P′, Figure 1. The contracted conformation consists of two hairpin motifs with tetra-loops, 5′·P·GTTG·P′·3′ and 5′·P·CTTC·P′·3′, connected by a 20T linker, while the elongated conformation is formed by base pairing the distant P and P′ regions. Two additional GC base pairs are also needed in the elongated conformation to compensate for the large entropic cost of the 20T hairpin loop and the 2T × 2T interior loop, as compared to the two

* To whom correspondence may be addressed. E-mail: herve.isambert@curie.fr.
† Physico-chimie Curie, CNRS UMR168, Institut Curie.
‡ Rowland Institute at Harvard, Harvard University.
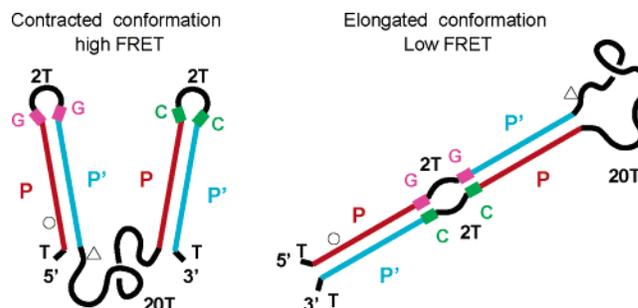
Figure 1. The DNA nanomechanical switch: The DNA switch sequence is 87 nt long: 5′·T·P·GTTG·P′·(T)$_{20}$·P·CTTC·P′·T·3′, including a P+P′ repeat, where P = 5′· CGACCTCAGCATCG·3′ and P′ = 5′·CGATGCTGAGGTCG·3′ are complementary regions, chosen such that no other complementary regions can pair on the sequence beyond two consecutive base pairs. Contracted (left) and elongated (right) conformations correspond to the two possible pairing combinations between P and P′. A pair of FRET dyes is used to distinguish the two conformations (Figure 2A) and study their spontaneous relaxation dynamics (Figure 3): Cy5 grafted on C5 (open circle) and TMR on T35 (open triangle).

small tetraloops of the contracted conformation. The structural switch between contracted and elongated conformations induces an atomic displacement from 20 Å (one helix diameter) to 110 Å (32 stacking base pairs) for the most distant exchanging base pairs, e.g., C2/G33. The two conformations are distinguished and studied combining fluorescence resonance energy transfer (FRET) measurements and electrophoresis separation on native polyacrylamide gels. Their relative thermodynamic stability can be tuned by varying the medium ionic strength, with the contracted conformation forming (>90%) under low ionic strength, while the elongated conformation is favored

Figure 2. A DNA switch two operating modes. (A) Thermodynamics control: The DNA switch is equilibrated in a low ionic strength solution (1x TAE plus 0.1 M NaCl, left) or in a high ionic strength solution (1x TAE plus 1 M NaCl, right): the two bands correspond to the contracted conformation (high FRET, left) and the elongated conformation (low FRET, right). (B) Folding kinetics control: Electrophoresis separation (12% 19:1 acrylamide−bisacrylamide native gel) demonstrates three successive switchings between contracted (upper band) and elongated (lower band) conformations under heating/cooling cycles in constant high ionic strength solution (1x TAE plus 1 M NaCl). Rapid cooling (R lanes, >100 °C/ms, see Methods) leads to 80 ± 3% of fast folding, contracted confirmations (ethidium bromide labeling), while moderate cooling rate (S lanes, <100 °C/s) leads to about 90% of lowest free-energy, elongatged conformations.

(>90%) under high ionic strength, Figure 2A. Both conformations coexist in equilibrium in a 1x TAE plus 0.25 M NaCl solution. Hence, the equilibrium conformation of the DNA switch can be controlled through changes in chemical environment, as similarly demonstrated for other examples of DNA nanomechanical devices[12−18] or for redox-sensitive synthetic switches[1,2] or for many natural protein or RNA switches both in vitro[19] and in vivo.[20] But the state of the present DNA nanomechanical switch can also be kinetically controlled under fixed chemical conditions, which could be more amenable to nanotechnology applications and integration.

This alternative operating mode relies on the difference in folding rates between the two conformations following heat denaturation. Figure 2B demonstrates the reversible switching between contracted and elongated conformations triggered by rapid or slow renaturation in high ionic strength solution. Rapid cooling rate (R lanes, >100 °C/ms, see Methods) induces 80 ± 3% of molecules to adopt the fast folding, contracted conformation, while moderate cooling rate (S lanes, <100 °C/s, manual handling) brings >90% of them into the lowest free-energy, elongated structure. Hence, folding kinetics control in high ionic strength solution can be used to rapidly and reversibly drive the DNA switch into its out of equilibrium, contracted state or into its equilibrium, elongated state. This result can be understood in terms of single-stranded DNA folding kinetics. The formation of DNA or RNA hairpin loops is known[21,22] to proceed at an average rate $k \simeq 10^4 - 10^5$ s^{-1} via stochastic nucleations of three to five consecutive base pairs along the helix length, followed by a rapid zipping of the neighbor base pair stacks ($\sim 10^7$ bp·s^{-1}). Larger transition loops lower the probability of helix nucleation and hence the folding rate of individual hairpins. Thus, short hairpin loops are expected to fully hybridize their helix before the first base pairs of much larger hairpin loops have a chance to nucleate. When short and large hairpin loops compete for common bases, as in the present case, conformations with short hairpin loops are kinetically favored,

irrespective of their thermodynamic stability, provided that the cooling rate around the melting temperature is fast enough. It should be around 100 °C/ms corresponding to a decrease of 10 °C within the hairpin nucleation time (10^{-4} s). In particular, manual handling is too slow to achieve rapid cooling rates and leads at best to 25% of kinetically trapped DNA switches. Hence, a custom-made instrument (see Methods) is necessary to trap $x = 80 \pm 3\%$ of the molecules. Interestingly, cooling rate control has also been used to kinetically favor self-assembly of small nanostructures instead of large polymeric networks,[23] although the dynamics of *inter*molecular assembly appeared considerably slower than the *intra*molecular folding dynamics of DNA switches (typical cooling rate[23] 0.001 vs 100 °C/ms here).

The observed 80% of kinetically trapped molecules is in good agreement with stochastic folding simulations using the algorithm Kinefold[24−26] with DNA base pair stacking free-energies.[27] It also agrees with a direct theoretical estimate of the kinetic partitioning between the four P/P′ pairing combinations, assuming that no other helix can nucleate under rapid cooling (see Methods). Experimentally, preventing alternative helices from competing for nucleation is actually critical: for instance replacing the two tetraloops GTTG and CTTC with triloops GTG and CTC, respectively, yields $x \simeq 60\%$, due to the competing nucleation of three base pairs between CTC and the GAG region from P′; substituting, as a control, the same tetraloops with GCG and CCC triloops, that cannot nucleate more than two consecutive base pairs anywhere on the sequence, rescues as expected kinetic partitioning $x \simeq 80\%$ (data not shown). Hence, efficient folding kinetics control is *only* achieved if the designed DNA switch[28,29] exhibits *both* a large, slow nucleating loop and *no* other alternative helix (longer than 2 bp) that could compete even transiently with the long designed helices under rapid cooling renaturation.

This peculiar sequence feature also greatly limits the number of possible intermediates along refolding pathways, thereby delaying the relaxation time between the two structures. Indeed, once folded, contracted and elongated conformations can coexist in any proportion for several weeks at room temperature. The relaxation time of the kinetically trapped, contracted conformation was directly measured by measuring the decay over time of the bulk FRET efficiency at various temperatures (Figure 3). We thus estimated the activation energy of spontaneous relaxation to be 70 kcal/mol. This amounts to about 30% of the contracted conformation enthalpy, which is comparable to an activation energy for the opening of eight base pairs. This is in good agreement with the relaxation process predicted by Kinefold[24−26] showing a four-way junction intermediate (Figure 4), analogous to the Holliday junction of genetic recombination.[30] It is the lowest free energy intermediate compatible with the unstacking of 8 bp. Driven and spontaneous transitions of the DNA switch under folding kinetics control are summarized on Figure 4.

Thanks to its simple design principle, this DNA switch can be easily adapted to meet particular specifications. Sequence and length of helix P/P′ can be modified to adjust
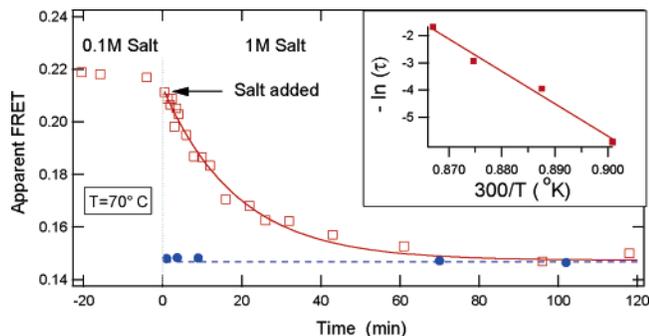
Figure 3. Spontaneous relaxation of the DNA switch. Spontaneous relaxation of the kinetically trapped, contracted conformation at constant temperature is studied using FRET measurements (with an excitation wavelenght of 501 nm), by first thermally equilibrating the DNA switch in this conformation (high FRET) in 1x TAE plus 0.1 M NaCl solution before suddenly raising the salt concentration, while keeping the temperature constant. The DNA switch then relaxes toward its new equilibrated state under high ionic strength, which corresponds to the elongated conformation (low FRET). The equilibration dynamics is followed over time under constant temperature for 73, 70, 65, and 60 °C, which leads to relaxation times of minutes to hours. The main figure displays the DNA switch relaxation at 70 °C (square) which eventually converges, as expected, toward the FRET level obtained by slowly cooling from 95 to 70 °C in 1x TAE plus 1 M NaCl solution (circle). A single exponential decay fits well the relaxation dynamics with a characteristic time τ. Figure inset shows that $\ln(\tau)$ varies linearly with $1/T$, where T is the temperature. The corresponding activation energy is 70 kcal/mol, while the contracted conformation enthalpy is estimated around 250 kcal/mol.[27]
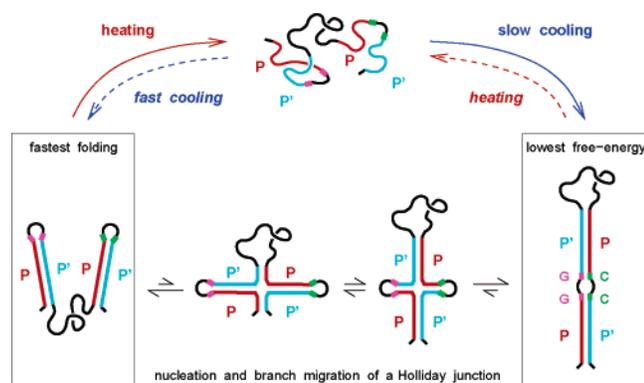
Figure 4. Driven and spontaneous transitions of the DNA switch. Heating and slow cooling (solid arrows) versus heating and fast cooling (dashed arrows) cycles drive the DNA switch back and forth between equilibrium, elongated conformation and out-of-equilibrium, contracted conformation through a denatured intermediate state in high ionic strength solution. Spontaneous relaxation operates on much longer time scales (beyond weeks at room temperature). The transition involves a nucleation step with simultaneous breaking of four base pairs in each hairpin helix and their rearrangement into an asymmetric Holliday junction, which is eventually resolved by spontaneous branch migration to form the lowest free-energy, elongated structure.

melting temperature, and the relative thermodynamic stability of contracted and elongated conformations can be fine-tuned by varying the solution ionic strength. While the dynamics of single molecules remains intrinsically stochastic, folding kinetics control can be improved, if needed, by using longer polynucleotide linkers (e.g., a 30T linker yields x ≃ 85%,

data not shown). We have checked the generality of this simple DNA switch design with a very different, 100 nt long sequence following the same design principle: 5′·P·GCGC· P′·(C)$_{40}$·P·GCCC·P′·3′, where P = 5′·TGATATTCTAAAT· 3′ and P′ = 5′·ATTTAGAATATCA·3′. While displaying similar folding kinetic partitioning (≃80%, data not shown), this DNA switch operates under much lower denaturation temperature (≃70 °C) due to the low G+C content of P and P′.

Folding kinetics control could be further improved, if needed, by constructing a series of noninteracting switches, (P$_i$GTTGP′$_i$ T$_{20}$P$_i$CTTCP′$_i$)$_n$ (e.g., average folding kinetics control is expected to increase from $x = 80\%$ to $x = 98\%$ with a series of nine independent DNA switches). Larger assemblies of individual switches could also generate larger cumulative displacements that can be directly probed using micromanipulation techniques.

A prospective use of such DNA switches under folding kinetic control can be to provide *rejuvenatable* "DNA-fuel" for DNA-driven nanodevices,[13−18] themselves relatively insensitive to fast cooling renaturation (due to multiple transiently competing helices and/or to the absence of large, slow nucleating loops in their sequence). Thus, regularly rejuvenated "DNA fuel" under folding kinetics control should enable a *continuous* driving of DNA-fueled nanodevices without the need for a chemical turnover of "fuel" and "waste" DNA strands in solution.

An attractive possibility to perform folding kinetics control on individual DNA switches is to use local heat sources.[31] In particular, there is no intrinsic limitation to achieve fast cooling rates locally at nanometer scales, as DNA folding kinetics is about 10 000 times slower than heat diffusion at these scales. Hence, DNA switches under folding kinetics control should function in an integrated environment with local heat sources inducing heating/cooling cycles of 10− 20 °C around melting temperature. Alternatively, light-sensitive DNA−azobenzene hybrids[32] or voltage addressable DNA switches[33] could also provide out-of-equilibrium driving mechanisms for DNA switches under constant temperature.

In summary, we have designed and experimentally studied DNA nanomechanical switches that can be driven back and forth between *out of equilibrium* and *equilibrium* states under *fixed* chemical conditions, by submitting them to fast and slow cooling rates, respectively. As prospects in nano-biotechnology[34] attract increasing interests, DNA switches operating under out of equilibrium conditions provide flexible, scalable alternatives to simultaneous chemical control of different DNA switches at equilibrium.

Materials and Methods. The Molecule. DNA sequences (see Figure 1 caption) were synthesized by IBA Germany and Eurogentec N.A. and PAGE purified. A Cy5 dye is coupled during synthesis to C5, and TMR succinimidyl ester is postcoupled to a primary amine group on T35. Uncoupled dyes are removed by column purification, four consecutive ethanol precipitations, and a final PAGE purification. The coupling efficiency is measured by absorption spectra and

corresponds to an average of 1 TMR and 0.6 Cy5 per DNA strand.

FRET Measurements. Bulk FRET measurements are performed on a Fluo-Time 100 (Pico Quant) instrument. The apparent FRET efficiency is calculated as $E = I_{acc}/I_{tot}$, where I_{acc} and I_{tot} are the acceptor intensity and total intensity, respectively. Although the measured FRET efficiency is biased by molecules lacking Cy5 dyes, this does not affect the measurements of the relaxation dynamics (Figure 3).

Rapid Cooling Procedure. Rapid cooling is achieved by a custom-made instrument consisting of a 100 μm $\times$ 100 μm capillary connected at one end to a high-pressure pump activated via a valve and at the other end to a reservoir of liquid propane at -180 °C. The central part of the capillary is immersed in a thermal bath regulated at a temperature ranging from 70 and 95 °C. The opening of the valve results in a rapid ejection (>100 m/s) of the DNA switch solution stored in the heated region of the capillary, into liquid propane reservoir, resulting in a cooling rate of >100 °C/ms.

Theoretical Estimate of Folding Kinetics Control. Kinetic partitioning between contracted and elongated structures can be estimated from the folding rates of the different P/P′ pairing combinations, assuming that no alternative helix can nucleate under rapid cooling. Larger transition loops lower the probability of hairpin nucleation and thereby their contribution to folding rate as $k \propto (2n + 1)^{-3\nu}$, where $2n + 1$ is the nucleation loop size and $\nu = 0.5-0.6$ is the Flory exponent for nonfolded polymer strands. Hence, the proportion of kinetically trapped, contracted conformations can be estimated as $x \simeq 2\Sigma_2^{10}(2n + 1)^{-3\nu}/(2\Sigma_2^{10}(2n + 1)^{-3\nu} + \Sigma_{10}^{40}(2n + 1)^{-3\nu}) = 80-90\%$ with $\nu = 0.5-0.6$.

References

(1) Bissell, R. A.; Córdova, E.; Kalfer, A. E.; Stoddart, J. F. *Nature* **1994**, *369*, 133−137.

(2) Collier, C. P.; et al. *Science* **2000**, *289*, 1172−1175.

(3) Brouwer, A. M.; et al. *Science* **2001**, *291*, 2124−2128.

(4) Sauvage, J.-P. *Science* **2001**, *291*, 2105−2106 and references therein.

(5) Seeman, N. C. *J. Theor. Biol.* **1982**, *99*, 237−247.

(6) Chen, J.; Seeman, N. C. *Nature* **1991**, *350*, 631−633.

(7) Mao, C.; Sun, W.; Seeman, N. C. *Nature* **1997**, *386*, 137−138.

(8) Shih, W. M.; Quispe, J. D.; Joyce, G. F. *Nature* **2004**, *427*, 618.

(9) Winfree, E.; Liu, F.; Wenzler, L. A.; Seeman, N. C. *Nature* **1998**, *394*, 539−544.

(10) LaBean, T.; et al. *J. Am. Chem. Soc.* **2000**, *122*, 1848−1860.

(11) Rothemund, P. W.; Papadakis, N.; Winfree, E. *PLoS Biol.* **2004**, *2*, 2(12): e424.

(12) Mao, C.; Sun, W.; Shen, Z.; Seeman, N. C. *Nature* **1999**, *397*, 144−146.

(13) Yurke, B.; Turberfield, A. J.; Mills, A. P., Jr.; Simmel, F. C.; Neumann, J. L. *Nature* **2000**, *406*, 605−608.

(14) Yan, H.; Zhang, X.; Shen, Z.; Seeman, N. C. *Nature* **2002**, *415*, 62−65.

(15) Turberfield, A. J.; Mitchell, J. C.; Yurke, B.; Mills, A. P., Jr.; Blakey, M. I.; Simmel, F. *Phys. Rev. Lett.* **2003**, *90*, 118102.

(16) Sherman, W.; Seeman, N. C. *Nano Lett.* **2004**, *4*, 1203−1207.

(17) Shin, J.-S.; Pierce N. A. *J. Am. Chem. Soc.* **2004**, *126*, 10834−10835.

(18) Liao, S.; Seeman, N. C. *Science* **2004**, *306*, 2072−2074.

(19) LeCuyer, K. A.; Crothers, D. M. *Proc. Natl. Acad. Sci. U.S.A.* **1994**, *91*, 333−3377.

(20) Winkler, W. C.; Nahvi, A.; Roth, A.; Collins, J. A.; Breaker, R. R. *Nature* **2004**, *428*, 281−286.

(21) Pörschke, D. *Biophys. Chem.* **1974**, *1*, 381−386.

(22) Bonnet, G.; Krichevsky, O.; Libchaber, A. *Proc. Natl. Acad. Sci. U.S.A.* **1998**, *95*, 8602−8606.

(23) Scheffler, M.; Dorenbeck, A.; Jordan, S.; Wüstefeld, M.; von Kiedrowski, G. *Angew. Chem., Int. Ed. Engl.* **1999**, *38*, 3312−3315.

(24) Isambert, H.; Siggia, E. D. *Proc. Natl. Acad. Sci. U.S.A.* **2000**, *97*, 6515.

(25) Xayaphoummine, A.; Bucher, T.; Thalmann, F.; Isambert, H. *Proc. Natl. Acad. Sci. U.S.A.* **2003**, *100*, 15310−15315.

(26) Xayaphoummine, A.; Bucher, T.; Isambert, H. *Nucleic Acid Res.* **2005**, *33*, 605−610.

(27) SantaLucia, J., Jr. *Proc. Natl. Acad. Sci. U.S.A.* **1998**, *95*, 1460−1465.

(28) Flamm, C.; Hofacker, I. L.; Maurer-Stroh, S.; Stadler, P. F.; Zehl, M. *RNA* **2001**, *7*, 254−265.

(29) Nagel, J. H. A. Ph.D. Thesis, Leiden University, 2003.

(30) Seeman, N. C.; Kallenbach, N. R. *Annu. Rev. Biophys. Biomol. Struct.* **1994**, *23*, 53−86 and references therein.

(31) Hamad-Schifferli, K.; Schwartz, J. J.; Santos, A. T.; Zhang, S.; Jacobson, J. M. *Nature* **2002**, *415*, 152−155.

(32) Asanuma, H.; Ito, T.; Yoshida, T.; Liang, X.; Komiyama, M. *Angew. Chem., Int. Ed. Engl.* **1999**, *38*, 2393−2395.

(33) Isambert, H. *C. R. Physique* **2002**, *3*, 391−396.

(34) *Nanobiotechnology: Concepts, Applications and perspectives*; Niemeyer, C. M., Mirkin, C. A., Eds.; Wiley: Weinheim, 2004.

NL052161C